Stratification Phenomena in Thin Liquid Films Containing Polyelectrolytes and Stabilized by Ionic Surfactants

César Márquez Beltrán, Samuel Guillot,† and Dominique Langevin*

Laboratoire de Physique des Solides, Bâtiment 510, Université Paris-Sud, 91405 Orsay Cedex, France

Received May 9, 2003; Revised Manuscript Received July 25, 2003

ABSTRACT: We have investigated the oscillations of the disjoining pressure, corresponding to film stratification, for foam films containing small concentrations of ionic surfactants and carboxymethylcellulose, an anionic polysaccharide. In water, this polyelectrolyte does not form surface complexes with AOT, an anionic surfactant. However, when mixed with cationic surfactants, in this case alkyltrimethylammonium bromides (C_nTAB), strong polymer−surfactant interactions create an enhanced coadsorption of both components at the air−water interface that strongly depends on surfactant concentration. We have found stratification phenomena whatever the nature of the surfactant. The oscillation period of the disjoining pressure varies with the polymer concentration as $C_p^{-1/2}$, and is close to the mesh size defined for semidilute polymer solutions. However, the dynamic properties of the liquid films and their stability are in turn very sensitive to the nature of the surfactant charge, as revealed from the behavior of the stratification kinetics.

1. Introduction

Many studies of foam films have been made in the recent years.[1−4] These studies contributed to the development of the classical DLVO theory of molecular forces. Surface forces, when counted per unit area, were called disjoining pressure Π by Derjaguin, who added to the classical DLVO forces (electrostatic double layer, van der Waals) a third and short-range steric repulsive interaction. In this way, the stability of the very thin *Newton black films*, made of surfactant bilayers, can be accounted for. If surfactant micelles are present in the solution, they are confined between film surfaces. When these surfaces are close enough, confinement gives rise to stratification during film drainage[5] and thus to oscillations of the disjoining pressure.[6] Stepwise thinning was also observed in films formed from aqueous concentrated dispersions of spherical latex particles,[7] aqueous solutions of vesicles[8] and giant micelles.[9] This stepwise thinning is associated with the formation of ordered structures inside the film. In the case of particles or micelles, the step size corresponds to the mean distance between them. Similar phenomena were observed when a polyelectrolyte was added to a surfactant solution.[10−15] In this case, the confinement of the polymer network also gives rise to a stepwise thinning of the film with a step size close to the mesh size ξ of the polymer network, as well as to oscillations in the disjoining pressure with the same period ξ.

Mixed aqueous solutions of polyelectrolytes and surfactants have attracted much interest[16] due to their use in industrial processes and to their biological relevance. Mixed aqueous solutions of polyelectrolytes and surfactants of opposite charge also possess unusual surface properties.[17,18] In such systems, polyelectrolyte charges play an important role still to be understood:[19,20] mixed surface layers are thicker than pure surfactant monolayers and could stabilize foam films. Mixed solutions containing small concentrations of cationic surfactants (alkyltrimethylammonium bromide C_nTAB) and flexible anionic polymer (polyacrylamide sulfonate, PAMPS, and polystyrenesulfonate, PSS: intrinsic persistence length $l_p^{int} \sim 1$ nm[21]) lead to stable thin films and stratification phenomena. Films made with the same surfactants and anionic polymers with a rigid backbone, such as xanthan ($l_p^{int} = 140$ nm in the double helix form[22]) or DNA ($l_p^{int} = 50$ nm[23]), were found to be unstable. Polyelectrolytes form surface complexes with oppositely charged surfactants which are *film stabilizing* if they are loosely packed as for PAMPS or PSS, but *film destabilizing* if they are more densely packed, as for xanthan or DNA.[24] For all polymers, stable films can be obtained with either nonionic or anionic surfactant solutions. In all cases,[11−15] the disjoining pressure Π oscillations and the step size Δh are independent of the surfactant type and scale with polymer concentration as $C_p^{-1/2}$. It has been found that Δh is comparable to the mesh size ξ of the semidilute polymer network, as expected theoretically.

In this paper, we present a study of films made from mixed solutions of carboxymethylcellulose (CarboxyMC), an anionic polysaccharide having an intermediate rigidity ($l_p^{int} \sim 5-10$ nm[25,26]), and various cationic (C_nTAB) or anionic (sodium dioctyl sulfosuccinate, AOT) surfactants. In this way, we can have films with or without polymer−surfactant complexes at their surface. The films made with cationic surfactants are stable enough, although less stable than those made with AOT. We have observed a stratification phenomenon, as for other polyelectrolytes,[10−15] independent of surfactant charge type. We have then investigated the stratification kinetics in order to find explanations of the differences in film stability observed with the different surfactants.

2. Experimental Section

2.1. Materials. Dodecyltrimethylammonium bromide (DTAB), tetradecyltrimethylammonium bromide (TTAB) and hexadecyltrimethylammonium bromide (CTAB) were obtained from Aldrich (purity better than 99%) and recrystallized three times before use from an acetone−ethanol (24:1) solution. The anionic surfactant dioctyl sulfosuccinate (AOT) was also purchased from Aldrich and used as supplied.

* To whom correspondence may be addressed.
† Present address: Biophysics Laboratory, Physik Department (E22), Technische Universität München, James-Frank-Strasse, 85748 Garching bei München, Germany.

10.1021/ma034599+ CCC: $25.00
Published on Web 10/07/2003

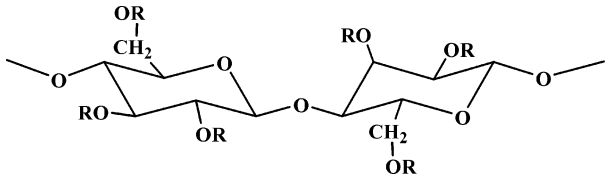

Figure 1. Schematic illustration of the repeating unit structure of sodium CarboxyMC: Glucose units are linked by β-1.4-linkages. R = −H or R = −CH_2COONa depending on the degree of substitution DS.

CarboxyMC is a water-soluble linear polymer, used in food, cosmetic, and pharmaceutical applications. Its preparation[27] leads to partial substitution of the 2-, 3-, and 6-hydroxyl groups by hydrophilic carboxymethyl groups (structure shown in Figure 1). The distribution of the substituted residues is nonuniform[28] because of the heterogeneous conditions used in the preparation similar to that of methylcellulose: CarboxyMC is a random block copolymer.[29] We used Blanose Sodium CarboxyMethylCellulose 12M31P, kindly supplied by Aqualon Hercules (minimum purity of 99.5% related to dry matter: CarboxyMC is known to be highly hydrated[30]). No further purification was done before use. Its substitution degree (average number of carboxymethyl groups per glucose unit) is DS = 1.23. With a monomer length of $b \approx 5$ Å[31] and a Bjerrum length in water of $l_B \approx 7$ Å, we expect counterion condensation ($b/l_B <$ DS). Furthermore, this condensation should not be uniform because of the nonuniform substitution.

Some experiments have been done with PAMPS, a random copolymer of acrylamide and acrylamidomethylpropanesulfonate, from SNF Floerger. The number fraction of charged monomers of the polymer used is 25%. With a monomer length of 2.5 Å, the average distance between charges is 7.5 Å, larger than the Bjerrum length; thus, no counterion condensation is expected for this polymer.

The mixed solutions were obtained by adding the polymer to the surfactant solutions and using deionized water (Millipore Milli-Q system). The polymer powder is dissolved while stirring for at least 8 h.

2.2. Surface Tension Measurements. Surface tension measurements were performed with two methods. The first one is the Wilhelmy method with an open frame, made of soldered platinum wires.[32] The frame is dipped into the solution and then lifted up: a liquid film is formed, and the lift force increases because of the weight of the film. The film drains by gravity and the force decreases until stabilization, after which the film generally breaks. The lift force is measured with an electromagnetic transducer. The surface tension γ is then obtained from the relation $\gamma = K\Delta V$, where ΔV is the difference of potentials measured before and after film breakage, and K is a calibration constant set with pure liquids (water, butanol). This method avoids the irreversible adsorption and wetting problems of the more classical Wilhelmy plate[33] but cannot be used when the film is too stable and does not easily break. Since this happened in our solutions (with cationic surfactants, slightly below CAC, see afterward) the axisymmetric drop shape analysis method was used, with a pendant drop tensiometer from IT Concept[34] (Longessaigne, France). An air bubble is formed on the tip of a J-shaped needle, fixed on a syringe, dipped into a thermostated cuvette filled with the solution. The volume of the bubble can be adjusted in a controlled way with the syringe, whose plunger is linked to a micrometer screw driven by a motor. This axisymmetric bubble is illuminated with a white light uniform source, and a CCD camera records its profile. The bubble shape is digitized and then analyzed with the Laplace−Young equation, which leads in particular to the surface tension. Typical accuracy of the two methods is 0.1 mN/m.

Surface tension does not vary significantly with temperature (typically 0.1 mN/m/°C), at least in the range where the experiments have been done (20−25 °C).

2.3. Surface Viscoelasticity. The drop tensiometer was also used to measure the surface compression elastic modulus of the mixed layers. For this purpose an air bubble, with a volume of about 9−11 μL, is periodically compressed and expanded at a periodicity of 10s and an amplitude in the range of 3.5−7 μL. Because the adsorbed mixed layers behave as insoluble ones, the elastic modulus exhibits a small frequency dependence and the measured elasticity is close to the Gibbs elasticity $E = A\partial\gamma/\partial A$, where A is the surface area.

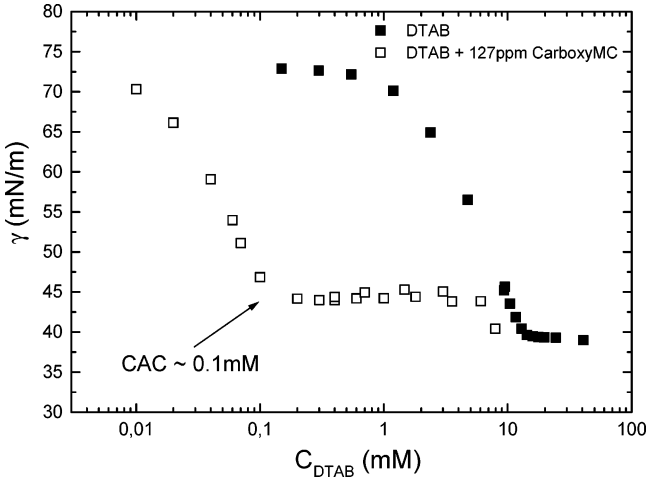

Figure 2. Variation of the equilibrium surface tension of DTAB/CarboxyMC mixed solutions (open symbols) and pure DTAB solutions (filled symbols), as a function of DTAB concentration (log units). Polymer concentration is 127 ppm. The CAC is about 0.1 mM.

2.4. Bulk Viscosity. The bulk viscosity of the solutions was measured by using capillary glass tubes (internal radius 0.54 mm and a Cannon-Fenske routine glass viscometers by Ever Ready Thermometer Co.). After pouring a fixed amount of solution in the viscometer, the solution and water flow times, t and t_0, were measured. Knowing water viscosity η_0, we can deduce the viscosity of our solutions with $\eta = \eta_0(t/t_0)$, neglecting corrections due to input and output effects.[35] The relative viscosity η_{rel}, is defined as $\eta_{rel} = \eta/\eta_0 = t/t_0$ and the specific viscosity is $\eta_{sp} = (\eta - \eta_0)/\eta_0$. Measurements were carried out at 25 ± 1 °C. The experimental accuracy is 0.02 cP.

2.5. Thin Film Balance and Disjoining Pressures. Disjoining pressures were measured with a modified version of the porous-plate technique.[36−38] This setup is fully described elsewhere:[6] single thin-liquid foam films are formed in the hole drilled through a fritted glass disk, onto which a glass capillary tube is fused. The free end of the capillary tube is at atmospheric pressure and the disk is enclosed in a pressurized cell. The pressure is regulated by a syringe pump, which allows us to change the pressure ΔP applied to the film. Once formed, the film thins because of the applied pressure, flattens and eventually reaches an equilibrium thickness. At equilibrium, ΔP is compensated by the disjoining pressure Π. The film thickness is measured by using Scheludko's microinterferometric method: a white light beam is focused onto the film, the reflected beam is filtered at 632 nm, and its intensity is measured with a photomultiplier. A chopper modulates the light beam intensity at 370 Hz and the photomultiplier signal is analyzed with a lock-in amplifier. Our equilibrium criterion is a constant reflected intensity during 20 min. The maximum applied ΔP is limited by film rupture. The evolution of the films during thinning is recorded on a computer. The image analysis has been done with Scion Image, software available on the Internet.[39]

3. Results and Discussion

3.1. Surface Tension and Viscosity. Equilibrium surface tensions of mixed solutions were measured as a function of surfactant concentration C_S. For a given surfactant concentration, surface tensions do not depend appreciably on polymer concentration C_p in the studied range.[40] Surface tensions are plotted in Figure 2 for

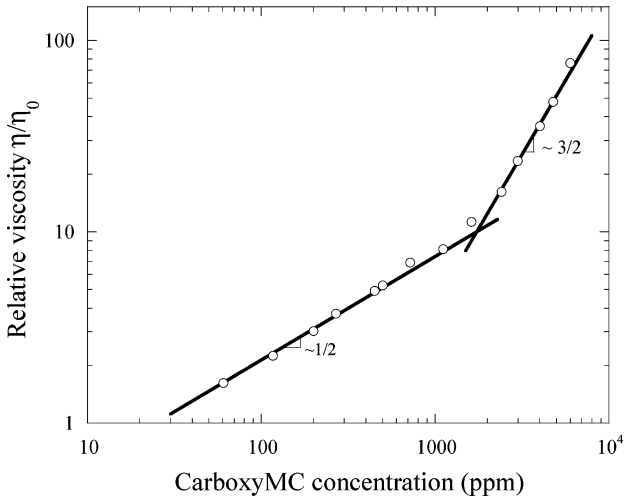

Figure 3. Relative viscosity of CarboxyMC aqueous solutions at 25 °C.

DTAB. We note that at very low surfactant concentrations, the surface tension of the mixed solutions is well below that of the pure surfactant solutions, underlining strong interactions between DTAB and CarboxyMC. The surface tension decrease results from surfactant and polymer coadsorption at the interface due to electrostatic interactions.[41] Above 0.1 mM, called the critical aggregation concentration (CAC), DTAB/CarboxyMC curve displays a plateau region, with $\gamma \approx 44$ mN/m. Above the CAC, surfactant−polymer complexes start to form in the solution; the CAC is usually lower than the surfactant critical micelle concentration (cmc) and the gap between both critical concentrations is a measure of the interaction strength between polymer and surfactant. Note that CarboxyMC is not surface-active at the air−water interface for the concentration at which the film studies have been made.[41] In the case of AOT, the surface tension is little affected by the presence of polyelectrolytes of the same charge, as it was previously shown.[10] The effect of the polymer is a mere change of ionic strength, leading to a small decrease of the cmc: no mixed polymer−surfactant layer is formed at the surface of the solution.

The relative bulk viscosity variation with polymer concentration for pure CarboxyMC aqueous solutions is shown in Figure 3. Below $C_e \approx 1740$ ppm (1 ppm $\equiv 10^{-6}$ g/cm^3), η_{rel} follows the Fuoss law: $\eta_{rel} \sim C_p^{1/2}$, which is a characteristic of the unentangled semidilute regime of flexible polyelectrolytes; above C_e, the relation $\eta_{rel} \sim C_p^{3/2}$ characterizes the entangled semidilute regime.[41] For most of our mixed film studies, we have used a polymer concentration of 1000 ppm in order to avoid the viscous entangled regime where films are gellike when using cationic surfactants.

In the mixed systems, we have worked below CAC, in order to avoid the presence of bulk aggregates. The bulk viscosities of the solutions studied are reported in Table 1. The viscosities with and without surfactant are however similar. Indeed, the surfactant concentration is below the CAC, and surfactant−polymer association in bulk is very limited. We show in Figure 4 that the viscosity changes drastically at larger surfactant concentrations (C_s > CAC) or when salt is added, due to a large conformational change of the polymer chains. As seen in the figure, cationic surfactants are more effective than simple salts to collapse polyelectrolytic chains.[41]

Table 1. Solution Viscosities

solutions	η (cP)
1000 ppm CarboxyMC	10.65
0.1 mM DTAB + CarboxyMC	10.15
0.1 mM TTAB + CarboxyMC	9.70
0.1 mM CTAB + CarboxyMC	9.80
0.1 mM AOT + CarboxyMC	9.68
0.1 mM DTAB + 1000 ppm PAMPS 25%	7.34

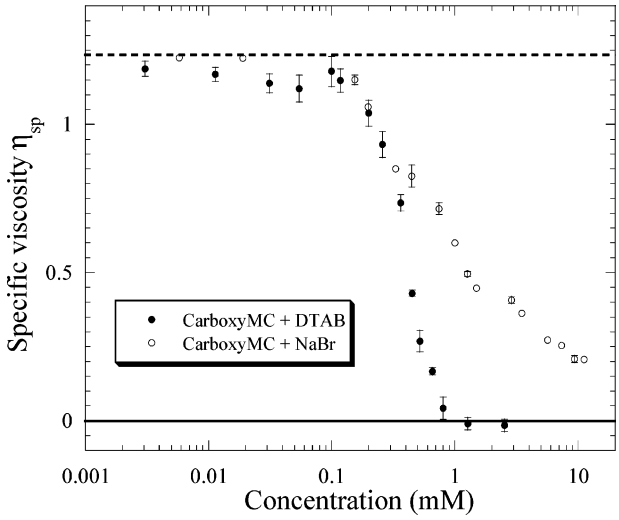

Figure 4. Specific viscosity $\eta_{sp} = (\eta - \eta_0)/\eta_0$ of 127 ppm CarboxyMC aqueous solutions as a function of added DTAB or NaBr concentration at 25 °C. The dashed line corresponds to a pure CarboxyMC solution, the baseline to water.

3.2. Stratification and Stability in Ionic Surfactants/CarboxyMC Liquid Films. The variation of the disjoining pressure Π with the film thickness h is shown in Figure 5 for AOT/CarboxyMC aqueous solutions with $C_{AOT} = 0.1$ mM and different polymer concentrations (500, 736, 2000, and 2990 ppm). Every disjoining pressure curve Π(h) was measured at equilibrium. At these polymer concentrations, the polymer alone does not adsorb at the film surfaces (the surface tension is equal to that of the surfactant solution). Jumps Δh in film thickness, i.e., stratification phenomena, were observed when increasing the applied pressure. When ΔP is continuously increased, the film thickness decreases along one branch of the disjoining pressure curve (see Figure 5). Above a certain pressure (top of a branch), domains of smaller thickness, corresponding to the next branch, nucleate and expand (this process will be described in more detail in section 3.3). When the domains fully cover the film, the corresponding new disjoining pressure branch is reached and so on until the film breaks in general above 1000 Pa. The minimum film thickness found was of the order of 20 nm. This phenomenon is not reversible: when ΔP is decreased, one stays in the same branch of the disjoining pressure curve and the film thickness does not increase much. The reproducibility of the transition pressure measurements is ±50 Pa. As seen in Figure 5, the number of jumps increases with polymer concentration: one jump at 500 and 736 ppm, two jumps at 2000 ppm and three jumps at 2990 ppm. For the last concentration, the two first jumps occur one after the other at the same low pressure. We also note that the stepsize (oscillation period) between two consecutive disjoining pressure branches is the same but decreases when polymer concentration increases: from 29 nm at 500 ppm to 10.3 nm at 2990 ppm. These films are *common black films*

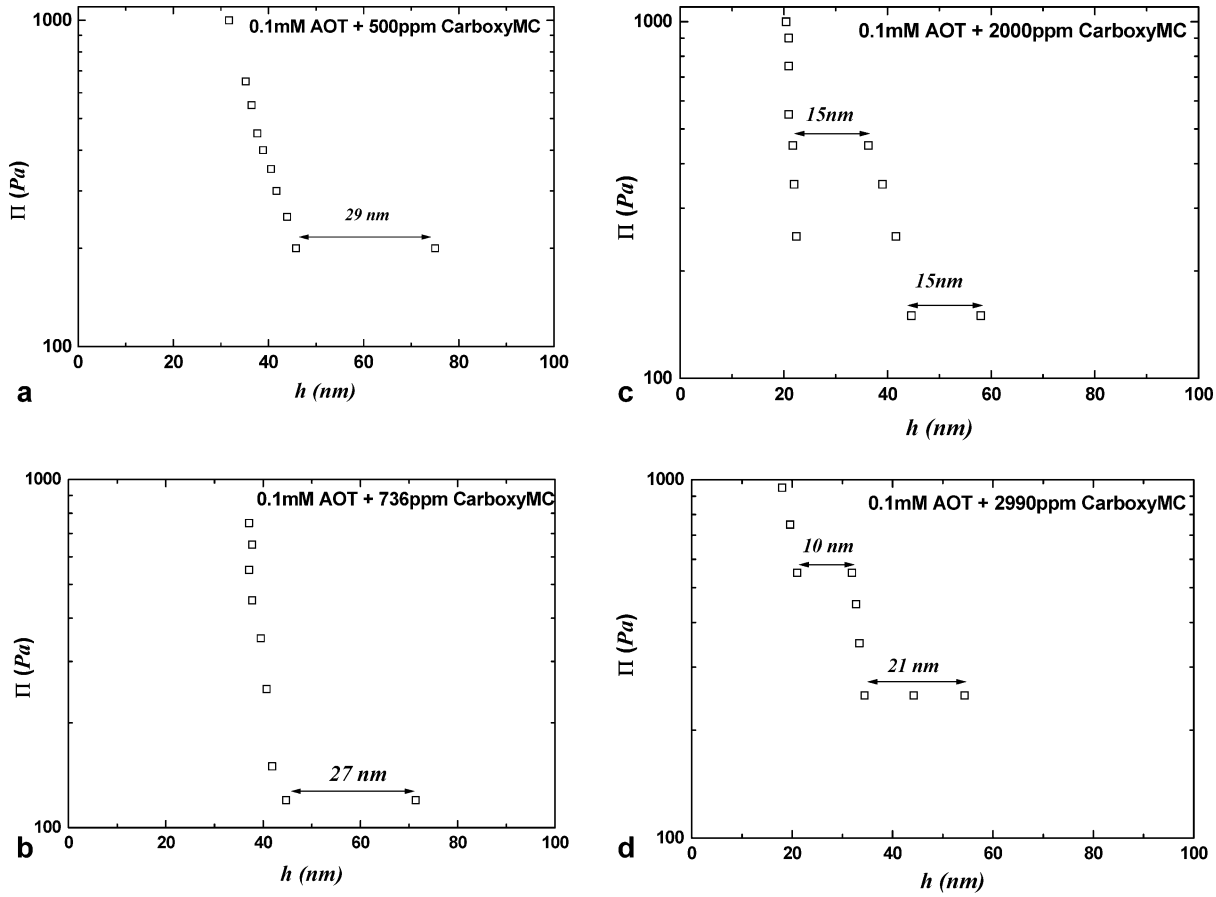

Figure 5. Disjoining pressure vs film thickness for mixed solutions containing 0.1 mM AOT and different concentrations of CarboxyMC: (a) 500, (b) 736, (c) 2000, and (d) 2990 ppm.

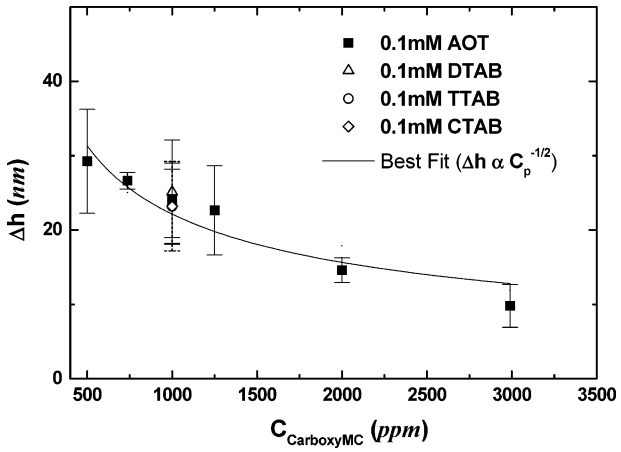

Figure 6. Measured jump size Δh as a function of polymer concentration for DTAB (triangles), TTAB (circles), CTAB (diamonds), and AOT (squares). The solid line correspond to a fit with $\Delta h \sim C_p^{-0.5}$.

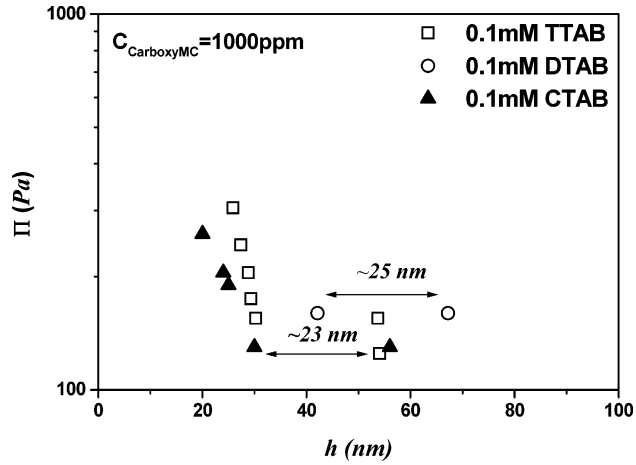

Figure 7. Disjoining pressure vs film thickness for mixed solutions of 0.1 mM C_nTAB and 1000 ppm CarboxyMC: DTAB (circles), TTAB (squares), and CTAB (triangles).

and still contain appreciable amounts of water.[1−4] This is often the case for this kind of systems, although *Newton black films* have been found in the poly(DADMAC)/APG system for example.[13]

Let us recall that, in semidilute solutions, the mesh size ξ of the polyelectrolyte network scales with polymer concentration as $\xi \sim C_p^{-1/2}$. As we see in Figure 6, the jump size Δh also varies as $C_p^{-1/2}$. This is as found earlier for both flexible and rigid polyelectrolytes.[12]

We have also studied liquid films containing CarboxyMC and cationic surfactants, in which complexes are present at the film surfaces. The disjoining pressure measurements for solutions containing 1000 ppm polymer and 0.1 mM surfactant are displayed in Figure 7. Stratification was observed in all C_nTAB systems for which the jump size was almost found the same (23 nm for TTAB and CTAB and 25 nm for DTAB). In the case of DTAB, the film breaks just after the first jump. Thus, films made with DTAB are less stable than those with TTAB or CTAB. The same behavior is observed with films made from the pure surfactant solutions: it is well-known indeed that the stability depends on the length of the hydrophobic surfactant tail.[42] The jump size for cationic surfactants is also the same as for the anionic surfactant AOT at $C_p = 1000$ ppm (see Figure

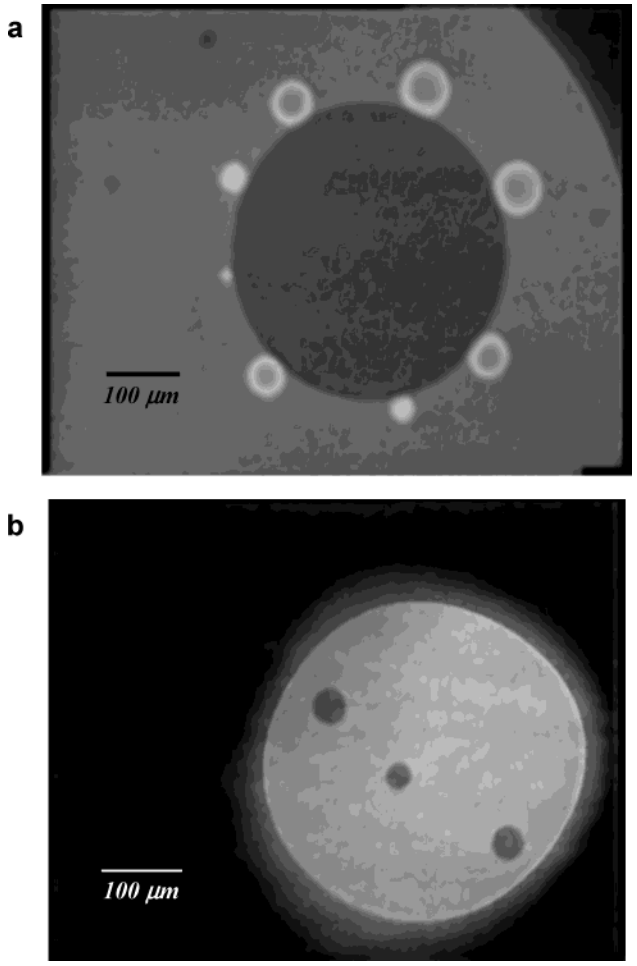

Figure 8. Images of horizontal thin films during film-thinning: (a) view of the stratification domain with rim instabilities, AOT/CarboxyMC solutions; (b) stratification domains in DTAB/CarboxyMCsolutions.

6). This is as found earlier for poly(styrenesulfonate) when using either DTAB or a neutral surfactant.[14] This is also consistent with the fact that the jump size is associated with the polymer network, and therefore should not be influenced by the surfactant type at the low concentrations used. We could not perform a systematic study with the cationic surfactants, by increasing the polymer concentration, for several reasons: the viscosity strongly increases, drainage becomes slow, asymmetric dimples are formed and move slowly toward the film border, and the film breaks before small thicknesses are reached. A further increase in C_p leads to gellike films that do not reach a plane-parallel state.

3.3. Stratification Kinetics. In this section, we present results on the expansion of isolated stratification domains. We have studied horizontal films formed by using fritted glass disks of 100 μm mean porosity. These studies were done using solutions containing 0.01 or 0.1 mM surfactant. At these concentrations, bulk viscosity is close to that of the pure polymer solution. Note that for a fixed surfactant concentration, the Debye length is the same in all the mixed solutions. To obtain reproducible results, we have studied stratified domains formed far from other nucleated ones and from the edge of the film meniscus.

In the case of AOT/CarboxyMC solutions, a rim is formed during domain expansion. This rim is unstable and breaks into droplets surrounding the domain (Rayleigh type of instability). These droplets, also observed in other foam films,[43] are thicker than the surrounding film and consequently reflect more light (Figure 8a). For C_nTAB/CarboxyMC solutions, no visible rim is seen around the dark spots, which seem quite flat (Figure 8b), although the image analysis reveals that a shallow rim might be present (of much smaller height than in the AOT case). The time dependence of the domain radius, $r(t) \sim t^{\nu}$, for all systems is shown in Figure 9.

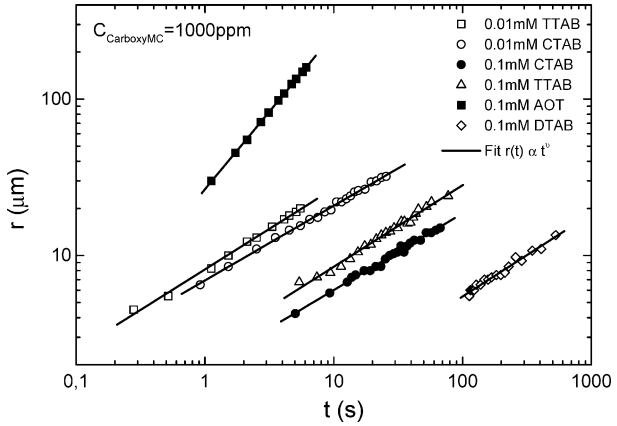

Figure 9. Time dependence of the stratification domain radius $r(t)$ for the AOT/CarboxyMC and C_nTAB/CarboxyMC systems. The solid lines correspond to fits with $r(t) \sim t$ for AOT and $r(t) \sim t^{1/2}$ for C_nTAB.

For AOT/CarboxyMC system, we have found the same linear law $r(t) \sim t$ as in previous studies[43] on liquid films made from concentrated polymer-free DTAB solutions ($C_s = 0.1$ M $\sim$ 7 times the cmc), in the last stages of the stratification process, when the films contain a very small number of micellar layers. The problem is an analogue to the one of dewetting of a liquid film on a solid (or liquid) surface. The expansion velocity $V = dr/dt$ is given by $V = V^*\theta^3$, with $V^* \sim (\gamma/\eta)^{1/2}$ and θ the contact angle between adjacent layers.[43,44] In the case of pure DTAB film stratification, this contact angle is small when the film contains a large number of layers, because the layers are similar, but θ increases when the number of layers decreases. The rim formation and rupture are instabilities taking place when the velocity is large enough,[45] meaning that the contact angle needs also to be large. This is probably why it is only observed for the last layers in the pure DTAB films. The velocity of expansion of the domains in the case of AOT/CarboxyMC solutions is 26 μm/s, comparable to those measured for the pure DTAB films.[43] It must be stressed that the kinetics does not involve here the expulsion of layers of micelles, but layers of the polymer network. Let us also note that the above theoretical velocity corresponds to domains where the rim has not been ruptured into droplets. It has however been noted by Reiter and co-workers that even after the occurrence of the instability, the domains also expand at constant velocity in liquids dewetting a solid surface.[46]

In the case of C_nTAB/CarboxyMC, the stratification kinetics resembles more that of the thicker pure DTAB films. No rim instability is observed and $r(t) \sim (4D_{\text{eff}}t)^{1/2}$ ($\nu \sim 0.5$): see Figure 9. We have studied here two surfactant concentrations, 0.01 and 0.1 mM, and we have found that the effective diffusion coefficient decreases with increasing surfactant concentration (Table 2).

A similar diffusion mechanism has been predicted and observed for the expansion of stratified PDMS drops on

Table 2. Power Law Exponents ν for the Variation of the Stratification Domain Radius vs Time and Effective Diffusion Coefficient D_{eff}

$C_p = 1000$ ppm	ν (± 0.01)	D_{eff} (10^{-8} cm^2/s)
0.01 mM TTAB	0.52	18
0.01 mM CTAB	0.48	11
0.1 mM TTAB	0.52	2
0.1 mM CTAB	0.49	1
0.1 mM DTAB	0.53	0.2
0.1 mM DTAB[43] (without polymer)		25

silicon substrates.[47,48] It was shown that D_{eff} can be written as

$$D_{eff} = \frac{h^3}{3\eta}\frac{\partial \Pi}{\partial h} \quad (1)$$

In the case of PDMS drops, the disjoining pressure is dominated by van der Waals forces and $D_{eff} = A_H/6\pi\eta h$, where A_H is the Hamaker constant. The stepsize being 0.7 nm, this leads to $D_{eff} \sim 1.5 \times 10^{-7}$ cm^2/s, for PDMS solutions with viscosities of 20 cP, about 100 times smaller than the measured values. It should be noted that the measured diffusion coefficient does not vary with bulk viscosity as predicted by eq 1, especially in conditions where the layer friction with the substrate is small, in which case D_{eff} was found independent of the bulk viscosity.[48] In our experiments, the disjoining pressures are controlled by the structural forces producing the oscillations and are different from van der Waals forces. The D_{eff} values for the mixed films are smaller than those of pure DTAB (Table 2), although the bulk viscosity is about 10 times larger for the mixed solutions and the stepsize is only 2−3 times larger for the mixed films (about 20 nm).

We have compared the kinetics observed for films containing 0.1 mM DTAB and a more flexible polymer (PAMPS). The viscosity of the solutions was here somewhat smaller (see Table 1). The expansion of domains followed a diffusive behavior, with an effective diffusion coefficient of $D_{eff} \sim 27 \times 10^{-8}$ cm^2/s, i.e., 100 times larger than with CarboxyMC at the same surfactant concentration. This large difference is difficult to rationalize.

Until now, we have not taken into account, in addition to the molecular forces, the surface elasticity and surface viscosity of the film surfaces. Surface elasticity is a measure of the energy stored in the surface layer as a result of an external stress, whereas surface viscosity is a measure of the speed of the corresponding relaxation process. This surface viscoelasticity might play a role in the stratification kinetics and explain the differences observed between anionic and cationic surfactants. The values measured for the elastic modulus are reported in Table 3. The moduli are larger for the mixed films with C_nTAB than with AOT because surfaces of AOT/CarboxyMC solutions are covered by only pure AOT monolayers. The C_nTAB/CarboxyMC solutions have therefore a more cohesive monolayer at the surface than those of AOT/CarboxyMC. This suggests that the stratification kinetic could be controlled in part by the viscous dissipation close to the film surfaces. This effect could partly explain the difference between the behavior of anionic and cationic surfactants in the stratification kinetics. However, the differences between the films made with DTAB, TTAB, and CTAB cannot be rationalized in this way, because the different moduli are similar.

Table 3. Real and Imaginary Parts of the Surface Dilational Modulus for Various Surfactant Concentrations as Obtained by the Oscillating Bubble Method with a Period of 10 s

$C_p = 1000$ ppm	surface dilational modulus (mN/m)	ϵ_r (mN/m)	ϵ_i (mN/m)
0.01 mM DTAB	29 ± 2	23 ± 1	4 ± 1
0.01 mM TTAB	48 ± 8	46 ± 8	10 ± 4
0.01 mM CTAB	48 ± 3	46 ± 4	9 ± 2
0.1 mM DTAB	40 ± 3	39 ± 3	11.4 ± 0.4
0.1 mM TTAB	37 ± 6	36 ± 6	7 ± 1.5
0.1 mM CTAB	43 ± 5	43 ± 6	7 ± 1
0.1 mM AOT	7 ± 2	6 ± 2	3 ± 0.3

4. Conclusions

We have found that the dynamic properties of the liquid films containing polyelectrolytes and in particular their stability are very sensitive to the nature of the surfactant. When cationic surfactants are added to the CarboxyMC solutions, a slow stratification is found, whereas the stratification is faster in the case of the anionic surfactant AOT. With AOT, the rim of the domain moves at constant velocity whereas the stratification with C_nTAB is of the diffusive type. The trends exhibited by the stratification kinetics are opposite to the trends in stability: the stratification is faster for the more stable films.

Further work is in progress in order to explain these differences and to analyze the results with appropriate theoretical models.

Acknowledgment. We thank Aqualon France for kindly supplying CarboxyMC Blanose type, Jean François Argillier at the Institut Français du Pétrole for the gift of PAMPS samples, and Claude Germain for his help with surfactants recrystallization. C.M.B. thanks CONACYT-Mexico, Consejo Nacional de la Ciencia y Tecnologia for a doctoral fellowship. This work has been supported in part by the ECOS-ANUIES project M00P3.

References and Notes

(1) Derjaguin, B. V. *Theory of stability of colloids and thin films*; Johnston, R. K., Translator; Consultant Bureau: New York, 1989.
(2) Verwey, E. J. W.; Overbeek, J. Th G. *Theory of stability of lyophobic colloids, the interaction of sol particles having and electric double layer*; Elsevier: New York, 1948.
(3) Scheludko, A. *Adv. Colloid Interface Sci.* **1967**, *1*, 391.
(4) Ivanov, I. B. *Thin Liquid Films, Fundamentals and Applications*; Surfactant Sciences Series, Vol. 29; Marcel Dekker: New York; 1988.
(5) Nikolov, A. D.; Wasan, D. T. *J. Colloid Interface Sci.* **1989**, *133*, 1.
(6) Bergeron, V.; Radke, C. J. *Langmuir* **1992**, *8*, 3020.
(7) Wasan, D. T.; Nikolov, A. D.; Kralchevski, P. A.; Ivanov, I. B. Colloids Surf. **1992**, *67*, 139.
(8) Bergeron, V. *Langmuir* **1996**, *12*, 5751.
(9) Espert, A.; v. Klitzing, R.; Poulin, P.; Colin, A.; Zana, R.; Langevin, D. *Langmuir* **1998**, *14*, 4251.
(10) Bergeron, V.; Langevin, D.; Asnacios, A. *Langmuir* **1996**, *12*, 1550.
(11) Asnacios, A.; Espert, A.; Colin, A.; Langevin, D. *Phys. Rev. Lett.* **1997**, *78*, 4974.
(12) v. Klitzing, R.; Espert, A.; Hellweg, T.; Colin, A.; Langevin, D. *Colloids Surf. A* **1999**, *149*, 131.
(13) Kolaric, B.; Jeager, W.; v. Klitzing, R. *J. Phys. Chem. B* **2000**, *104*, 5096.
(14) v. Klitzing, R.; Espert, A.; Colin, A.; Langevin, D. *Colloids Surf. A* **2001** *176*, 109.
(15) Bergeron, V.; Theodoly, O.; Tan, J. S.; Ober, R.; Williams, C. E. *Langmuir* **2001**, *17*, 4910.
(16) Goddard, E. D.; Ananthapadmanabhan, K. P. *Interactions of Surfactants with Polymers and Proteins;* CRC Press: Boca Raton, FL, 1993.

(17) Goddard, E. D. *J. Colloid Interface Sci.* **2002**, *256*, 228.
(18) Langevin D. *Adv. Colloid Interface Sci.* **2001**, *89*, 467.
(19) Diamant, H.; Andelman, D. *Macromolecules* **2000**, *33*, 8050.
(20) Sokolov, E.; Yeh, F.; Kohkhlov, A.; Grinberg, V.; Chu, B. *J. Phys. Chem. B.* **1998**, *102*, 7091.
(21) Barrat, J. L.; Joanny, J. F. *Adv. Chem. Phys.* **1996**, *94*, 1.
(22) Milas, M.; Rinaudo, M.; Duplessix, R.; Borsali, R.; Lindner, P. *Macromolecules* **1995**, *28*, 3119.
(23) Hagerman, P. J. *Annu. Rev. Biophys. Chem.* **1988**, *17*, 265.
(24) Stubenrauch, C.; Albouy, P. A.; v. Klitzing, R.; Langevin, D. *Langmuir* **2000**, *16*, 2036.
(25) Rinaudo, M. *Cellulose and Cellulose Derivatives: Physicochemical Aspects and Industrial Applications*; Kennedy, J. F., Philips, G. O., Williams, P. O., Piculell, L., Eds.; Woodhead Publishing Limited: Cambridge, U.K., 1995; p 257.
(26) Hoogendam, C. W.; de Keizer, A.; Cohen Stuart, M. A.; Bijsterbosch, B. H.; Smit, J. A. M.; van Dijk, J. A. P. P.; van der Horst, P. M.; Batelaan, J. G. *Macromolecules* **1998**, *31*, 6297.
(27) Nussinovitch, A. *Hydrocolloid Applications. Gum technology in the food and other industries*, 1st Ed.; Blackie Academic & Professional: London, 1997; Chapter 6, Cellulose Derivatives, pp 105−124.
(28) Bhattacharjee, S. S.; Perlin, A. S. *J. Polym. Sci.: Part C* **1971**, *36*, 509.
(29) Arisz, P. W.; Kauw, H. J. J.; Boon, J. *J. Carbohyd. Res.* **1995**, *271*, 1.
(30) Koda, S.; Hasegawa, S.; Mikuriya, M.; Kawaizumi, F.; Nomura, H. *Polymer* **1988**, *29*, 2100.
(31) Meyer, K. H.; Misch, L. *Helv. Chim. Acta* **1937**, *20*, 234.
(32) Mann, E. K. Ph.D. Thesis, Paris, 1992.
(33) Mann, E. K.; Langevin, D. *Langmuir* **1991**, *7*, 1112.
(34) Labourdenne, S.; Gaudry-Rolland, N.; Letellier, S.; Lin, M.; Cagna, A.; Esposito, G.; Verger, R.; Rivière, C. *Chem. Phys. Lipids* **1994**, *71*, 163.
(35) Whorlow, R. H. *Rheological Techniques;* J. Wiley & Sons: New York, 1980. Bagley, E. B. *J. Appl. Phys.* **1957**, *28*, 624.
(36) Mysels, K. J.; Jones, M. N. *Discuss. Faraday. Soc.* **1996**, *42*, 42.
(37) Exerowa, D.; Scheludko, A. *C. R. Acad. Bulg. Sci.* **1971**, *24*, 47.
(38) Exerowa, D.; Kolarov, T.; Khristov, Khr. *Colloids Surf.* **1987**, *22*, 171.
(39) Scion Image Beta 4.0.2, 2000 Scion Corporation, www.scioncorp.com.
(40) Asnacios, A.; Langevin, D.; Argillier, J. F. *Macromolecules* **1996**, *29*, 7412.
(41) Guillot, S.; Delsanti, M.; Désert, S.; Langevin, D. *Langmuir* **2003**, *19*, 230.
(42) Bergeron, V. *Langmuir* **1997**, *13*, 3474.
(43) Sonin, A. A.; Langevin, D. *Europhys. Lett.* **1993**, *22*, 271.
(44) de Gennes, P.-G. *Phys. Amphiphilic Layers* **1987**, *34*, 64.
(45) Bergeron, V.; Jimenez-Laguna, A. I.; Radke, C. J. *Langmuir* **1992**, *8*, 3027.
(46) Reiter, G.; Sharma, A. *Phys. Rev. Lett.* **2001**, *87*, 166103.
(47) de Gennes, P.-G. *C. R. Acad. Sci. Paris* **1984**, *298*, 475; de Gennes, P.-G.; Cazabat, A.-M. *C. R. Acad. Sci. Paris* **1990**, *310*, 1601.
(48) Valignat, M. P.; Oshanin, G.; Villette, S.; Cazabat, A.-M.; Moreau, M. *Phys. Rev. Lett.* **1998**, *80*, 5377.

MA034599+